Supporting Information

Gasser et al. 10.1073/pnas.1321600111

SI Materials and Methods

Molecular Biology. For expression in *Escherichia coli*, the DNA encoding residues 1–506 of *Deinococcus radiodurans* bacterial phytochrome (*Dr*BPhy; UniProt BPHY_DEIRA) was amplified by PCR from the *D. radiodurans* type strain DSM 20539 (DSMZ). The gene encoding residues 553–941 of *Homo sapiens* cAMP/cGMP-specific phosphodiesterase 2A (*Hs*PDE2A; UniProt PDE2A_HUMAN) was synthesized with *E. coli*-adapted codon use (Geneart). The fusion construct LAPD+2 between *Dr*BPhy (amino acids 1–506) and *Hs*PDE2A (amino acids 553–941) was generated by restriction cloning in the pET-28c vector (Novagen, Merck). Subcloning into the pASK43 vector (IBA GmbH) using NheI/HindIII furnished LAPD+2 with a C-terminal hexahistidine tag. Light-activated phosphodiesterase (LAPD), the C24A mutant of LAPD, and LAPD linker variants were generated by site-directed mutagenesis using the QuikChange protocol (Invitrogen, Life Technologies). For studies in eukaryotic cells, genes of *Dr*BPhy and *Hs*PDE2A with *H. sapiens*-adapted codon use were obtained by gene synthesis (Geneart) or by amplification from a full-length cDNA clone of *Hs*PDE2A (imaGenes GmbH), respectively. The LAPD fusion construct with *H. sapiens*-adapted codon use was constructed in pASK43 as described above. For expression in CHO cells, the LAPD gene was subcloned under the control of a CMV promoter in pEGFP-N1 (Clontech) using NheI/NotI, thereby removing the EGFP tag on the vector. For RNA production for zebrafish experiments, the LAPD gene was cloned into the pGEM vector (Promega). All constructs were confirmed by DNA sequencing (GATC Biotech).

Protein Expression and Purification. The pASK43 expression plasmids encoding LAPD variants were transformed into *E. coli* BL21 (DE3) cells carrying the pKT270 plasmid (1), which encodes *Synechocystis* sp. heme oxygenase 1. Five hundred milliliters of LB was inoculated and incubated at 37 °C and 225 rpm (New Brunswick Innova 43R incubator shaker); protein expression was induced at an OD at 600 nm of ∼0.5 by adding 0.2 $\mu g \cdot mL^{-1}$ anhydrotetracycline, 1 mM isopropyl-β-D-thiogalactopyranoside, and 500 μM δ-aminolevulinic acid hydrochloride. After incubation for 18 h at 16 °C and 225 rpm (New Brunswick Innova 43R incubator shaker), cells were harvested by centrifugation and suspended in lysis buffer [50 mM Tris·HCl (pH 8.0), 20 mM NaCl, 20 mM imidazole, Complete Ultra protease inhibitor mixture (Roche), lysozyme, DNaseI]. Upon lysis by sonication, the cleared lysate was incubated in the presence of 100 μM biliverdin hydrochloride (Frontier Scientific) and 5 mM Tris-(2-carboxyethyl)-phosphine hydrochloride for 1 h at 4 °C. Following incubation, the lysate was purified over a gravity-flow Co^{2+}-nitrilotriacetic acid affinity chromatography column (HisPur Cobalt Resin; Thermo Scientific). His-tagged protein was eluted with buffer containing 200 mM imidazole, dialyzed against storage buffer [20 mM Tris·HCl (pH 8.0), 20 mM NaCl, 5 mM β-mercaptoethanol], and concentrated with a centrifugal filter device (10,000-Da size cutoff; Corning). Purified samples were analyzed by gel electrophoresis, where protein was stained with Coomassie Brilliant Blue, and covalently bound biliverdin was monitored via zinc-induced fluorescence (2). Expression and purification were performed at 4 °C in the dark or under dim green light. Protein concentration was determined by absorption spectroscopy with an Agilent 8453 UV-visible spectrophotometer (Agilent Technologies) using an extinction coefficient of 45,700 $M^{-1} \cdot cm^{-1}$ at the isosbestic point (724 nm) (3). The degree of biliverdin incorporation was determined by absorption spectroscopy of LAPD denatured in 6.5 M guanidine hydrochloride (4). The amount of chromophore was calculated using the extinction coefficient for free biliverdin at 388 nm of 39,900 $M^{-1} \cdot cm^{-1}$; notably, the absorption of biliverdin at this wavelength is little affected by denaturant addition (4). The amount of protein was calculated based on absorption at 280 nm after correcting for the contribution of biliverdin absorption at this wavelength.

In Vitro Activity Assays. Catalytic activity was measured at 25 °C in solutions containing 5 nM enzyme (LAPD or variants), 50 mM Tris·HCl (pH 8.0), 8.3 mM $MgCl_2$, 50 $\mu g \cdot mL^{-1}$ BSA, and 7 mM β-mercaptoethanol (5). Reactions were started by adding 25–2,000 μM cAMP or cGMP. Experiments were conducted under dark conditions (i.e., dim green light) or under illumination 2 min before and during the reaction. A bandpass filter (ThorLabs) was used to select a wavelength of 690 nm (FWHM, 10 nm; power, 3.3 $mW \cdot cm^{-2}$) or light-emitting diodes of 455 nm (FWHM, 20 nm; power, 75 $mW \cdot cm^{-2}$) and 850 nm (FWHM, 30 nm; power, 28 $mW \cdot cm^{-2}$). For white-light irradiation, a tungsten halogen cold-light source was used (150 W, DCR III; Schott). Aliquots taken after 15 s to 2 min of reaction time were immediately transferred to 95 °C to stop the reaction and to denature the PDE enzyme. Samples were cleared by centrifugation and filtration (0.2-μm pore size, Chromafil; Macherey–Nagel), and were analyzed by HPLC (Knauer). cGMP and GMP were separated on a C18 reverse-phase column (Supelco; Sigma–Aldrich) using isocratic conditions [100 mM potassium phosphate (pH 5.9), 4 mM tetrabutylammonium iodide, 10% (vol/vol) methanol] (6). cAMP and AMP were separated on a C18 reverse-phase column using gradient elution [buffer A: 25 mM potassium phosphate (pH 5.5); buffer B: 94 mM potassium phosphate (pH 5.5); 25% (vol/vol) acetonitrile; gradient: 0–70% B within 12.5 min] (7). Elution was monitored by absorbance at 253 nm; data were evaluated with Clarity Chrom (Knauer) and Origin (Origin Lab Corp.). Peak areas were integrated and assigned to the educt cyclic NMP and the product NMP based on retention times of the corresponding standard compounds. To account for loading differences, we used an internal standardization procedure, where the product amount is normalized to the sum of the educt and product amounts.

In Vivo Activity Assays in CHO Cells. To generate a stable LAPD reporter cell line, a precursor atrial natriuretic peptide (ANP) reporter cell line (8) was cotransfected with a LAPD construct and the pcDNA3.1/hygro vector (Invitrogen). Stably transfected clones were obtained by hygromycin selection (0.4 $mg \cdot mL^{-1}$) and were characterized by ANP stimulation plus/minus illumination. One clonal cell line was selected for further experiments and is referred to as the LAPD reporter cell line. In parallel, a stable WT PDE2A reporter cell line was generated as before (9). Cultures of LAPD and PDE2A cell lines were grown in black 384-well microtiter plates (9). Following inoculation of ∼2,500 cells per well, the plates were incubated for 24 or 48 h at 37 °C and 5% (vol/vol) CO_2. Supernatant culture medium was discarded, and cells were loaded with 5 $\mu g \cdot mL^{-1}$ coelenterazine (CAS no. 55779-48-1; P. J. K. GmbH) in Ca^{2+}-free Tyrode solution [20 mM Hepes (pH 7.4), 130 mM NaCl, 5 mM KCl, 1 mM $MgCl_2$, 4.8 mM $NaHCO_3$] for 3 h at 37 °C and 5% (vol/vol) CO_2. ANP stimulation was performed in the absence or presence of the PDE2-specific inhibitor BAY 60-7550 (Axxora Life Sciences, Inc.). Both ANP and the inhibitor were dissolved in Ca^{2+}-free Tyrode solution containing 1 $mg \cdot mL^{-1}$ BSA. During incubation for 10 min, cells were either illuminated with white light (3,000

LX) or kept in the dark. Aequorin luminescence was measured immediately before and for 50 s following addition of Ca^{2+} ions to a final concentration of 3 mM using a CCD camera (Hamamatsu Corporation) in a light-tight box. The prism software (GraphPad Software, Inc.) was used for curve fitting and calculation of the EC_{50}, which are given as mean ± SEM (n = 6–7).

In Vivo Activity Assays in Zebrafish Embryos. Zebrafish husbandry and maintenance were carried out under standard conditions (10). All experiments performed in this study were conducted according to the guidelines of the German animal welfare law and were approved by the Animal Protection Office of the Max Planck Institute of Medical Research/University of Heidelberg. LAPD RNA was prepared from the pGEM-LAPD vector using the mMessage mMachine T7 Ultra Kit (Ambion), and 2 pg of this RNA was injected into WT (AB and TL zebrafish strains) embryos at the one-cell stage. Embryos were maintained in the dark and were dechorionated manually at 1 d postfertilization. Both uninjected controls and LAPD-injected embryos were treated with 300 μM forskolin and illuminated for 5 h with 625-nm light (1.1 $mW{\cdot}cm^{-2}$) or 950-nm light (270 $\mu W{\cdot}cm^{-2}$). Embryos were collected immediately afterward and instantly homogenized in 0.1 M hydrochloric acid. After centrifugation, the supernatants were stored at −20 °C. The cAMP levels were determined using a cAMP ELISA kit according to the manufacturer's protocol (Enzo Life Sciences); actual cAMP concentrations were calculated based on known cAMP standards.

Structural Analysis. Using LSQKAB (11), the structures of *Hs*PDE2A [Protein Data Bank (PDB) ID code 3IBJ (5)] and *Pseudomonas aeruginosa* bacterial phytochrome (*Pa*BPhy) [PDB ID code 3C2W (12)] were superposed with regard to their cGMP PDE/adenylyl cyclase/FhlA (GAF)-B– and phytochrome (PHY)-specific domains, respectively. The rotation matrix for this transformation is [[0.023, 0.446, −0.895], [0.247, −0.870, −0.427], [−0.969, −0.211, −0.130]], and the translation vector is [−59.5 Å, 30.2 Å, 105.8 Å]. Based on this superposition, a model of LAPD+2 was generated, where the orientation of the helices directly C-terminal of the *Pa*BPhy PHY domain was manually adjusted to achieve good overlap with the helices N-terminal of the *Hs*PDE2A catalytic domain. Molecule graphics were prepared with PyMOL (Schrödinger, LLC).

1. Mukougawa K, Kanamoto H, Kobayashi T, Yokota A, Kohchi T (2006) Metabolic engineering to produce phytochromes with phytochromobilin, phycocyanobilin, or phycoerythrobilin chromophore in Escherichia coli. *FEBS Lett* 580(5):1333–1338.
2. Berkelman TR, Lagarias JC (1986) Visualization of bilin-linked peptides and proteins in polyacrylamide gels. *Anal Biochem* 156(1):194–201.
3. Wagner JR, et al. (2008) Mutational analysis of Deinococcus radiodurans bacteriophytochrome reveals key amino acids necessary for the photochromicity and proton exchange cycle of phytochromes. *J Biol Chem* 283(18):12212–12226.
4. Shu X, et al. (2009) Mammalian expression of infrared fluorescent proteins engineered from a bacterial phytochrome. *Science* 324(5928):804–807.
5. Pandit J, Forman MD, Fennell KF, Dillman KS, Menniti FS (2009) Mechanism for the allosteric regulation of phosphodiesterase 2A deduced from the X-ray structure of a near full-length construct. *Proc Natl Acad Sci USA* 106(43):18225–18230.
6. Ryjenkov DA, Tarutina M, Moskvin OV, Gomelsky M (2005) Cyclic diguanylate is a ubiquitous signaling molecule in bacteria: Insights into biochemistry of the GGDEF protein domain. *J Bacteriol* 187(5):1792–1798.
7. Díaz Enrich MJ, Villamarín JA, Ramos Martínez JI, Ibarguren I (2000) Measurement of adenosine 3′,5′-cyclic monophosphate and guanosine 3′, 5′-cyclic monophosphate in mussel (Mytilus galloprovincialis lmk.) by high-performance liquid chromatography with diode array detection. *Anal Biochem* 285(1):105–112.
8. Wunder F, Woermann A, Geerts A, Milde M (2013) Pharmacological characterization of receptor guanylyl cyclase reporter cell lines. *Eur J Pharmacol* 698(1-3):131–136.
9. Wunder F, Gnoth MJ, Geerts A, Barufe D (2009) A novel PDE2A reporter cell line: Characterization of the cellular activity of PDE inhibitors. *Mol Pharm* 6(1):326–336.
10. Westerfield M (2000) *The Zebrafish Book: A Guide for the Laboratory Use of Zebrafish* (Danio rerio) (Univ of Oregon Press, Eugene, OR), 4th Ed.
11. Kabsch W (1976) A solution for the best rotation to relate two sets of vectors. *Acta Crystallogr A* 32:922–923.
12. Yang X, Kuk J, Moffat K (2008) Crystal structure of Pseudomonas aeruginosa bacteriophytochrome: Photoconversion and signal transduction. *Proc Natl Acad Sci USA* 105(38):14715–14720.

Fig. S1. Structure-based alignment of coiled-coil linkers in *Hs*PDE2A and BPhys. (*A*) Structure-based alignment of the coiled-coil linker region of *Pseudomonas aeruginosa* BPhP (*Pa*BPhP), *Deinococcus radiodurans BPhP (Dr*BPhP), and *Hs*PDE2A (compare Fig. 1*C*) provides design prescriptions for LAPD+2, whose sequence is indicated by the arrow. (*B*) The LAPD construct, variants LAPD−1 through LAPD−4 and variants LAPD+1 through LAPD+7 were obtained by consecutively deleting residues from the linker or by inserting residues into the linker (compare Table S1).

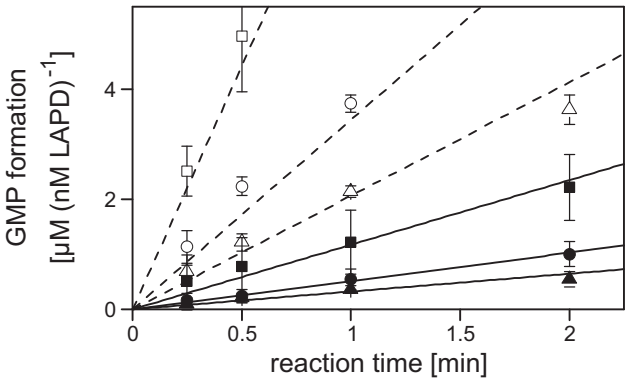

Fig. S2. Red-light–activated cGMP hydrolysis by LAPD illustrated in a magnified view of Fig. 2*B*. Integration of peak areas from HPLC analysis yields initial reaction velocities, v_0, at concentrations of 50 μM (▲), 100 μM (●), and 500 μM (■) cGMP. LAPD activity is enhanced under 690-nm light (open symbols) compared with dark conditions (closed symbols). Data are mean ± SD of two measurements; lines denote linear fits to determine v_0 values.

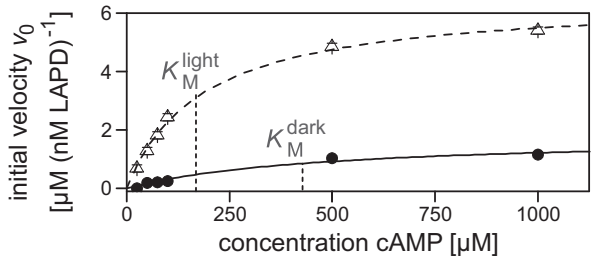

Fig. S3. Red-light–activated cAMP hydrolysis by LAPD. LAPD displays Michaelis–Menten kinetics for cAMP hydrolysis in both darkness (●, solid line) and under 690-nm light (Δ, dashed line). The v_0 values were determined by least-squares fitting and are reported as mean ± asymptotic SE. The maximum velocity, v_{max}, is increased from 1.8 ± 0.3 μM·min^{-1} (nM LAPD)$^{-1}$ in the dark to 6.5 ± 0.2 μM·min^{-1} (nM LAPD)$^{-1}$ under 690-nm light; the K_m value is decreased from 470 ± 170 μM in the dark to 180 ± 20 μM under 690-nm light. Lines denote fits to hyperbolic functions.

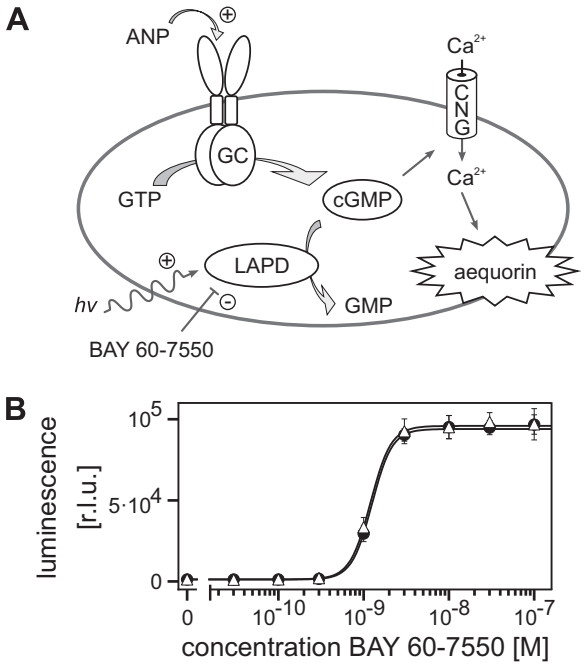

Fig. S4. CHO cells expressing WT *Hs*PDE2A do not respond to light. (*A*) Schematic of the LAPD reporter CHO cell line that constitutively expresses the ANP receptor and a cGMP-gated cyclic nucleotide–gated (CNG) channel. ANP addition triggers intracellular cGMP synthesis and opening of the CNG channel. Resultant calcium influx enhances luminescence of an aequorin reporter. Hydrolysis of cGMP by LAPD hence results in channel closing and decreased luminescence. (*B*) CHO cells stably transfected with WT *Hs*PDE2A instead of LAPD show no light dependence of PDE activity. Cells were stimulated with 10 nM ANP in the presence of different concentrations of the PDE2-specific inhibitor BAY 60-7550. Symbols denote reporter cell bioluminescence measured under dark (●) or light (Δ) conditions. Luminescence data are reported as relative light units (r.l.u.) and represent mean ± SEM of six to seven measurements; lines denote fits to hyperbolic functions.

Table S1. Fusion constructs between *Dr*BPhy and *Hs*PDE2A

	Residues from	
Construct	*Dr*BPhy	*Hs*PDE2A
LAPD−4	1–506	559–941
LAPD−3	1–506	558–941
LAPD−2	1–506	557–941
LAPD−1	1–506	556–941
LAPD	1–506	555–941
LAPD+1	1–506	554–941
LAPD+2	1–506	553–941
LAPD+3	1–507	553–941
LAPD+4	1–508	553–941
LAPD+5	1–509	553–941
LAPD+6	1–510	553–941
LAPD+7	1–511	553–941